

Soil profile analysis based on the identification of the bevametric parameters using a cone penetrometer

Rania Majdoubi,¹ Lhoussaine Masmoudi,¹ Abderrahmane Elharif²

¹LCS Laboratory; and ²Mechanical Laboratory, Faculty of Sciences, Mohammed V University in Rabat, Morocco

Abstract

The navigation in deformable soil is related to determining traction and motion resistance via the soil strength. This strength is a function of parameters usually estimated using the bevameter tool. However, this tool is not usually available, hence using another tool called a cone penetrometer. This study developed a new relationship to estimate the bevameter parameters. This relation combines all bevameter parameters; (shear strength and load penetration parameters) with a cone index measurement. This

equation is compared to another equation existing in the literature that uses only the load penetration parameters as a function of cone index and then validated using experimental data obtained from waterways experiment station (WES). The result shows that our equation is optimal compared to others existing in the literature. Finally, this equation is used to find all bevametric parameters of the soil inside the greenhouse strawberries.

Correspondence: Rania Majdoubi, LCS Laboratory, Faculty of Sciences, Mohammed V University in Rabat, Morocco.
E-mail: rania_majdoubi@um5.ac.ma

Key words: Bevametric parameter; characterisation of the soil; cone index; penetration parameters; shear parameters.

Acknowledgements: the authors of this paper are thankful to the Ministry of Higher Education and Scientific Research of Morocco (MESRSFC) and to the National Centre for Scientific and Technical Research of Morocco (CNRST) for financing this project, and to the Public Laboratory of Tests and Studies (LPEE) for providing the required material for the tests and the experimental study.

Funding: this research was conducted and funded by the Ministry of Higher Education and Scientific Research of Morocco (MESRSFC) and the National Center for Scientific and Technical Research of Morocco (CNRST).

Conflict of interest: the authors declare no potential conflict of interest.

Ethical approval: this article does not contain any studies with human participants or animals performed by any of the authors.

Received for publication: 20 August 2021.

Accepted for publication: 10 July 2022.

©Copyright: the Author(s), 2022

Licensee PAGEPress, Italy

Journal of Agricultural Engineering 2022; LIII:1262

doi:10.4081/jae.2022.1262

This article is distributed under the terms of the Creative Commons Attribution Noncommercial License (by-nc 4.0) which permits any non-commercial use, distribution, and reproduction in any medium, provided the original author(s) and source are credited.

Publisher's note: All claims expressed in this article are solely those of the authors and do not necessarily represent those of their affiliated organizations, or those of the publisher, the editors and the reviewers. Any product that may be evaluated in this article or claim that may be made by its manufacturer is not guaranteed or endorsed by the publisher.

Introduction

The robot's navigation in deformable soil like agricultural soil presents a big difficulty in traversability in some places (Molari *et al.*, 2015). These problems can be seen both in terms of surface shape (discontinuities, 3D relief, rock density) and the physical characteristics of the soil (loose soil, non-cohesive soil, sand, scree). These types of complex environments require locomotion systems with high mobility and crossing capacity. In the literature, a distinction is made between wheeled robots (Mei *et al.*, 2019), tracked robots (Dong *et al.*, 2016), walking robots (Hereid *et al.*, 2016), and hybrid robots (Ando *et al.*, 2017). The control of such robots requires the correct evaluation of the soil strength on which the robot evolves. Hence, the soil parameters such as cohesion, pressure sinking modules, and friction angle are identified by using several methods as defined in Ruiz (2015).

Navigation in a rough environment supposes two phases to study the behaviour of the wheel/soil systems (Li *et al.*, 2017; Wright *et al.*, 2017; Rios *et al.*, 2017; Rania *et al.*, 2022). The first step is ground modelling, which corresponds to studying the soil reaction under various solicitations, and then the ground characterisation. The second step corresponds to the interaction between the wheel and the soil. It supposes a study of the wheel, which mean modelling the contact geometry and its deformation. It should be noted that there are several methods for modelling the behaviour of the wheel/soil system. In the literature, these methods are classified into three main classes, among which we cite; the empirical methods as waterways experiment station (WES) detailed in Station (1964) and Smith (1986). NATO Reference Mobility Model (NRMM), which is based on soil characterisation as found in Next-Generation NATO Reference Mobility Model Development (2018), and the characterisation using cone penetrometer in order to evaluate the mobility of the vehicle as elaborated in (Livneh and Livneh, 2013). The analytical method is based on a physical model for the wheel/soil interaction; in this case, the soil parameter modelling is based on a semi-empirical model using the soil behaviour, as well as the use of the bevameter instrument in the experiment, as found in Bekker 1969. And finally, the theoretical method the finite element method (FEM) based on the soil parameters obtained experimentally using the Plastic Deformation Model of the soil as found in Nowatzki, 1978.

The paper carried out, discusses a very important issue related to navigation in a rough environment. Hence, it includes determin-

ing soil parameters based on empirical and analytical methods using the bevameter tool. However, this latter is difficult to get in the open environment. Hence, we will determine the bevametric soil parameters using the cone penetrometer tool. The specification of this paper remains in using only one equation that includes all these parameters, contrary to the equations found in the literature, which enables finding load penetration parameters using one equation and then finding shear strength parameters using another equation. Hence, this paper is organised as follows. In section two, we start by introducing the classical method using a bevameter instrument and the cone penetrometer tool; in section three, we propose a new relationship between all bevametric parameters and the cone index, which will be compared to the existing method found in the literature as presented in section four. Section five is dedicated to applying the proposed equation inside a didactical greenhouse strawberry to find all soil parameters. And finally, we summarize this paper with a conclusion and future work.

Introduction

The classical method using a bevameter instrument

The bevameter is a device intended to measure the soil properties established in the Bekker equation (Bekker, 1969). This instrument produces the vehicle sinking while moving over a deformable surface changing the tire surface's traction. This test has two modalities, one specific to penetration resistance via the penetration of the bevameter plate and the other specific to shear resistance via the shear ring of the bevameter. These tests are detailed as follows.

Penetration test

This test allows for predicting the load-bearing capacity of the soil by using at least two deformation plates of different sizes; usually, three rectangular or circular plates of width or diameter respectively (b_1 , b_2 , and b_3) as shown in Figure 1A. Let the coefficient K defined by Bekker as the pressure measured in the plate at a penetration depth of 2.54 cm.

K has different values at each plate size and considered as a function of K_c , K_{ϕ} , and b_i , as shown in Equation 1.

$$K = \frac{K_c}{b_i} + K_{\phi} \quad /i = 1 \text{ ou } 2 \text{ ou } 3 \quad (1)$$

This equation provides the values of K_c , K_{ϕ} , using, two pressure measurements from the bevameter pressure plate. The ground sinking exponent, n , is the tangent of the slope angle obtained from the relationship between the sinking and the pressure during the test.

Shear test

This test predicts the shear surface strength through a shear ring or an annular shear plate, as shown in Figure 1B. The ring is placed on the ground with a normal load applied and rotated at a constant speed. The values of c and ϕ are found graphically and algebraically by solving simultaneous equations using the Mohr-Coulomb equation presented as follows (Johnson *et al.*, 1983):

$$\tau = c + \sigma \tan(\phi) \quad (2)$$

where:

τ is shear strength, (KPa); c is cohesion, (KPa); σ is normal load, (KPa); ϕ is the angle of internal friction, (Degrees).

The method using a cone penetrometer

The cone penetrometer consists of a steel shaft mounted with a conical tip to control the force and the position of the cone, as shown in Figure 1C and detailed by Wong in Bekker (1969). The cone is pressed through the soil at a constant speed, whose penetration resistance is observed. This technique (cone penetrometer) was developed during the Second World War by the WES of the American army to obtain reliable and rapid information about the soil encountered. The measurement identified using this instrument is called the cone index I_c . Two parameters can be distinguished, and the first is related to the soil penetration resistance, such as K_c , K_{ϕ} , and n . The second is the shear strength parameters such as c and ϕ . These parameters are usually measured by the bevameter tool. However, this tool remains challenging to get in the open environment. Therefore, some authors have developed equations that allow estimating the bevametric parameters with the help of a cone penetrometer tool via a cone index measurement (Janosi 1959). In this context, Janosi, Rohani, and Baladi (Janosi 1959; Rohani and Baladi, 1981) have developed a relationship that allows finding the Bavametric parameters as described below.

Penetration resistance parameter

These parameters are K_c , K_{ϕ} , and n . They are determined using the equation that relates the bevametric parameters to the cone index

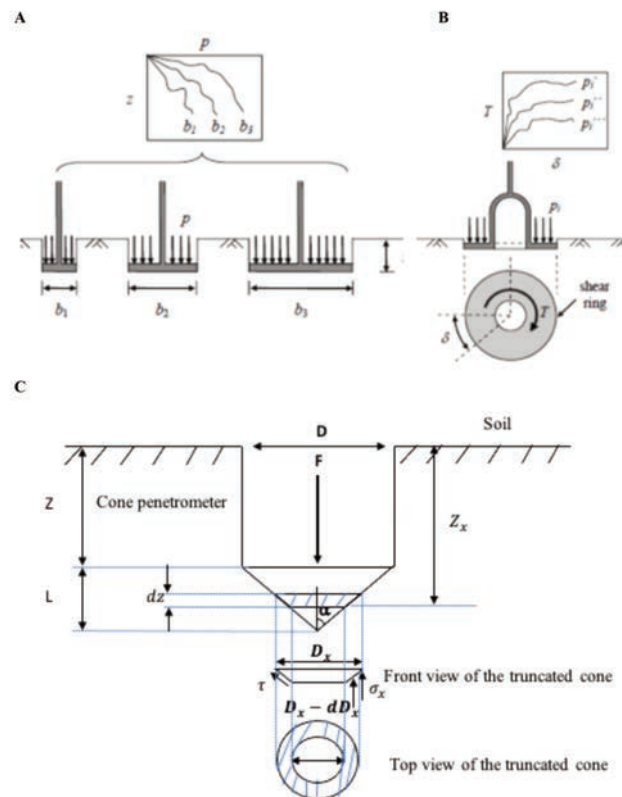


Figure 1. A-B) Schematic of the bevameter tool; C) cone penetrometer in its equilibrium.

as developed by Janosi (Janosi 1959) and shown in Equation 3:

$$I_c = 2\pi \tan(\alpha) \left[\frac{K_c}{n+1} ((Z+H)^{n+1} - (Z)^{n+1}) \right] + 4 \tan(\alpha) K_\phi \left[\frac{(Z+H)^{n+2}}{(n+2)(n+1)} + \frac{(Z)^{n+2}}{(n+1)} - \frac{(Z+H)Z^{n+1}}{(n+1)} \right] \quad (3)$$

where: I_c is the cone index, (KPa); K_c is the cohesion module, (KN/mⁿ⁺¹); K_ϕ is the friction module, (KN/mⁿ⁺²); n is the sinkage exponent; Z is the depth of the top of the cone to the surface, (m); H is the height of the cone, (m); α is the vertical angle of the cone, (Degree).

To find the values of K_c , K_ϕ and n , it is necessary to identify a relationship between two of these parameters according to the cone index I_c using experimental data found in the literature like WES as found in Station (1964) and Smith (1986) and deduce the third one from the Equation 3.

Shear strength parameters

These parameters are c and ϕ , which are determined using the method elaborated by Rohani and Baladi (Rohani and Baladi, 1981), who compared the amount of normal strength applied to the cone with the expansion of a series of spherical cavities expansion as elaborated by Vesic (Vesic, 1981). This assimilation is necessary to find the equation linking the bevametric shear strength parameters and the cone index, as shown in the following equation:

$$I_c = 6G_a^m \left(\frac{1+\sin(\phi)}{1-\sin(\phi)} \right) \left(\frac{\tan(\alpha)+\tan(\phi)}{\tan(\alpha)\tan(\phi)} \right) A - c \tan(\phi) \quad (4)$$

In which:

$$A = \frac{(c + (Z+H)\gamma \tan(\phi))^{3-m} - (c + (Z+H)\gamma \tan(\phi) + (2-m)H\gamma \tan(\phi)) (c + Z\gamma \tan(\phi))^{2-m}}{(2-m)(3-m)(H\gamma \tan(\phi))^2}$$

$$m = \frac{4\sin(\phi)}{3(1+\sin(\phi))}$$

where: ϕ is the angle of internal friction, (Degrees); γ is the density of the soil, (KN/m³); c is cohesion, (KPa).

Rohani and Baladi (1981) propose the expression of the shear module G_a , which varies according to the depth Z , as shown in Equation 5:

$$G_a^m = 0.5 \left(A + \frac{1-B e^{\beta Z}}{1+B e^{\beta Z}} \right) G \quad (5)$$

$$G = \frac{1230 (2.97 - e)^2}{1 + e} (\sigma_0)^{0.5}$$

The constants A , B , and β are related to the characteristics of the cone used in WES (Smith, 1986) ($H=3.7592$ cm, $D=2.02946$ cm and $2\alpha=30^\circ$), we get $A=0.986$, $B=100$ and $\beta=0.216$ cm⁻¹ and σ_0 is the ambient strength, where $\sigma_0 = 6.89476$ KPa. Therefore, the void ratio e is defined as follows:

$$e = \frac{G_s \gamma_w}{\gamma_d} - 1 \quad (6)$$

$\gamma_w = 49.92 \text{e}10 \text{KN/m}^3$ is the weight by volume of the water. In most soils, $2.65 < G_s < 2.69$, we take as an average $G_s=2.67$. γ_d is the weight by volume of hard granules, for dry soils $\gamma_d = \gamma$, then

Equation 6 is simplified to Equation 7 as follows:

$$e = \frac{166.6}{\gamma} - 1 \quad (7)$$

Therefore:

$$G = \frac{1230 (3.97 - \frac{166.6}{\gamma})^2}{166.6} \gamma \quad (8)$$

In order to find the values of c and ϕ , we should determine a relation between one of these parameters as a function of the cone index I_c and deduce the second from Equation 4.

Proposed method

This approach provides all bevametric parameters simultaneously using an instrument called a cone penetrometer (Geotechnical, 1991). It has the same concept as Janosi and Rohani (Janosi 1959; Rohani and Baladi, 1981). But the difference is that this method uses a unique equation to give us all bevametric parameters simultaneously.

Figure 1C shows a cone penetrating deformable soil. The cone index is the pressure value, and it depends on soil shear and compression characteristics. To find F , it is necessary to consider the stability of the truncated cone element impregnated in the soil. The vertical force F is divided into two forces, one relative to soil compression σ_x acting on the truncated conical surface element dS , and the other to soil shear strength τ acting on the same surface element dS . In this case, the vertical force applied to the truncated cone is defined in Equation 9.

$$dF = (\tau + \sigma_x \tan(\alpha)) dS \quad (9)$$

The shear pressure τ is defined using the following equation (Bekker, 1969):

$$\tau = c + \sigma_x \tan(\phi) \quad (10)$$

From Equation 10, the Equation 9 becomes:

$$dF = (c + \sigma_x (\tan(\alpha) + \tan(\phi))) dS \quad (11)$$

The pressure σ_x is developed by the Terrestrial Locomotion Laboratory, which developed many empirical equations. For example, one of these equations that represents the load-deflection profile is expressed in Equation 12, as defined by Bekker (1969).

$$\sigma_x = \frac{(K_c + K_\phi) Z^n}{D_x} \quad (12)$$

The lateral area of the truncated cone is defined in Equation 13:

$$dS = \pi D_x dz \quad (13)$$

From Figure 1C, we obtain Equation 14:

$$D_x = \frac{D}{L} (Z + H - Z_x) \quad (14)$$

From Equations 12, 13, and 14, Equation 11 becomes:

$$dF = \pi ((\tan(\alpha) + \tan(\phi)) (K_c + \frac{D}{L} (Z + H - Z_x) K_\phi) Z_x^n + c \frac{D}{L} (Z + H - Z_x)) dz \quad (15)$$

The overall force F is obtained by integrating Equation 15 between Z and $(Z+L)$ bounds. Hence, we obtain Equation 16:

$$F = \pi ((\tan(\alpha) + \tan(\theta)) \int_Z^{Z+L} (K_c + \frac{D}{L}(Z+L-Z_x)K_\theta) Z_x^n dz + c \frac{D}{L} \pi \int_Z^{Z+L} (Z+L-Z_x) dz) \tag{16}$$

After integrating, we obtain Equation 17:

$$F = \pi ((\tan(\alpha) + \tan(\theta)) [\frac{K_c}{n+1} ((Z+L)^{n+1} - (Z)^{n+1}) + \frac{D}{L} K_\theta [\frac{((Z+L)^{n+2} - (Z)^{n+2} - L(n+2)Z^{n+1})}{(n+2)(n+1)}]] + \frac{\pi DL}{2} c) \tag{17}$$

The cone index I_c is obtained from the expression of F using Equation 18.

$$I_c = \frac{4F}{\pi D^2}$$

Hence, we get Equation 19:

$$I_c = \frac{4}{D^2} ((\tan(\alpha) + \tan(\theta)) [\frac{K_c}{n+1} ((Z+L)^{n+1} - (Z)^{n+1}) + \frac{D}{L} K_\theta [\frac{((Z+L)^{n+2} - (Z)^{n+2} - L(n+2)Z^{n+1})}{(n+2)(n+1)}]] + \frac{2L}{D} c) \tag{19}$$

From Figure 1C, we obtain Equation 20:

$$D = 2L \tan(\alpha) \tag{20}$$

Then,

$$I_c = \frac{4}{D^2} ((\tan(\alpha) + \tan(\theta)) [\frac{K_c}{n+1} ((Z+L)^{n+1} - (Z)^{n+1}) + 2 \tan(\alpha) K_\theta [\frac{((Z+L)^{n+2} - (Z)^{n+2} - L(n+2)Z^{n+1})}{(n+2)(n+1)}]] + \frac{1}{\tan(\alpha)} c) \tag{21}$$

This equation allows finding a relationship between all bevametric parameters K_c , K_θ , n , c , and θ as a function of the cone index I_c .

Results and discussion

To validate the found bevametric equation, we compare Janosi's equation defined in Equation 3 vs the proposed equation defined in Equation 21, using the sand experiment data obtained from the WES as detailed in Smith (1986). The cone penetrometer used to obtain the experimental data by WES has the following characteristics:

$$L = 0.0254 \text{ m}$$

$$\alpha = \frac{30}{2} = 15^\circ$$

Using the MPa as a unit of the cone index I_c , Janosi's equation (Equation 3) becomes:

$$I_c = 0.001625 [\frac{K_c}{n+1} ((Z+0.0254)^{n+1} - (Z)^{n+1}) + 0.517 K_\theta [(\frac{(Z+0.0254)^{n+2}}{(n+2)(n+1)} + \frac{(Z)^{n+2}}{n+1} - \frac{(Z+0.0254)Z^{n+1}}{n+1}]]] \tag{22}$$

And the proposed equation (Equation 21) becomes:

$$I_c = 20.408(0.26 + \tan(\theta)) [\frac{K_c}{n+1} ((Z+0.0254)^{n+1} - (Z)^{n+1}) + 0.536 K_\theta [\frac{((Z+0.0254)^{n+2} - (Z)^{n+2} - 0.0254(n+2)Z^{n+1})}{(n+2)(n+1)}]] + 0.003732c \tag{23}$$

These two equations allow finding a relationship between the bevametric parameters and the cone index.

In order to find the relationship between the penetration parameters, we need other equations. For this purpose, the experimental data given by WES (Smith, 1986) using sandy soil at an average depth of 0 to 0.1524 m are plotted as shown in the following figures (Figures 2 and 3A-C).

It can be seen from the graphs generated using sandy soil data obtained from the WES (Smith, 1986) that the range of variation of penetration resistance varies between 0.1 MPa and 0.6 MPa. And the cohesion modulus varies while increasing the penetration resistance and varies between 0.1 KN/mⁿ⁺¹ and 36 KN/mⁿ⁺¹. The same remark is available for the friction modulus and friction angle, where the variation range of friction modulus is between 460 KN/mⁿ⁺² and 3300 KN/mⁿ⁺², and the friction angle is between 29.4 and 32 degrees. All these three parameters measured experimentally can be approximated by a linear curve, called the tendency line based on the least square algorithm, whose equations are given below:

$$K_c = 37.867 I_c - 3.5335 \tag{24}$$

$$K_\theta = 2157.5 I_c + 481.5 \tag{25}$$

$$\theta = 3.371 I_c + 29.66 \tag{26}$$

In this case (sandy soil), the cohesion coefficient is fixed at $c = 0$.

The Excel solver tool is used for non-linear optimisation. Hence, we find the sinking exponent n as a function of the cone index using both Janosi's equation and the proposed equation.

Figure 3D shows the graphs of the sinkage exponent n as a function of the cone index obtained experimentally during the resolution of these equations [(Janosi's equation (Equation 22) and the proposed equation (Equation 23)] using the solver tool.

It can be seen in the graph above that the estimation of sinking exponent n , obtained from the proposed equation (Equation 22), is better than the one estimated by Janosi's method (Equation 23).

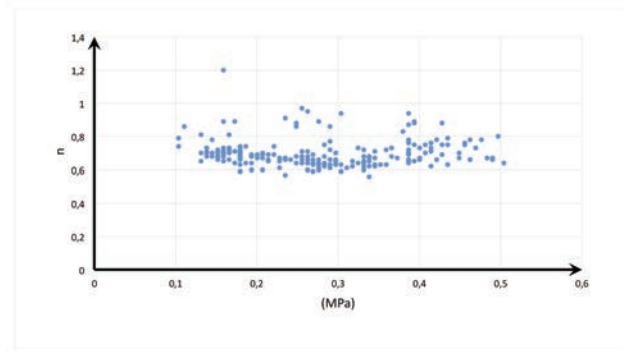


Figure 2. Experimental sinkage exponent versus cone index.

When we compare the two methods against the sinking exponent obtained experimentally from (Smith, 1986), it can be said that the proposed equation is more optimal concerning Janosi's equation.

Application inside a didactical greenhouse strawberry

Field description and measurement

During this study, data were collected from the soil to find the values of the bevametric parameters; [penetration resistance parameters (K_c , K_ϕ and n) and shear parameters (c , ϕ)] using the proposed equation given in Equation 21. In addition, measurements were taken inside the didactical greenhouse strawberry in the Faculty of Sciences in Rabat, which will be the area of testing the agricultural mobile robot (Majdoubi *et al.*, 2020; Majdoubi *et*

al., 2021; Majdoubi and Masmoudi, 2021; Majdoubi *et al.*, 2021; Ma'Arif *et al.*, 2021).

The cone index as a function of sinking depth was measured using a dynamic penetrometer as shown in Figure 4, in which the cone base area was 20 cm², a cone apex angle of 60°, and the height of the cone was 25 mm. The penetrometer was pushed through the ground with the help of hammering, driving, lifting, and ram-pulling equipment (a 64 kg cylindrical mass with a circular or square cross-section and a shearing). The measurements were taken at ten different areas along the robot's path in the greenhouses, as shown in Figure 5. At each area, measurements were taken at three areas chosen arbitrarily, at intervals of 30 mm to a depth of 1m. In addition, the soil was sampled using 50 mm diameter drill bits in the same depth range at five different areas picked arbitrarily from each area, as shown in Figure 6. Finally, the soil samples were weighed and oven-dried at 105°C for 24 hours and reweighed to determine the dry bulk density and moisture content, as shown in Table 1.

The samples were sent to a commercial laboratory for soil texture analysis, as shown in Table 2.

Figure 7A shows the average experimental data obtained at ten areas in the rows across the field inside the didactical strawberry greenhouse.

We notice in the graph that the cone index varies while descending to a given depth, this variation is either upward or downward, and it implies the presence of several layers at a given depth where several criteria may have occurred, such as clay fraction, moisture... also this measure varies while changing the area inside the greenhouse. The range of variation is defined between 0.4 MPa and 3 MPa. However, there is an aberrant measured point at the surface of the soil in area 10, which is due to measurement error during the experimentation.

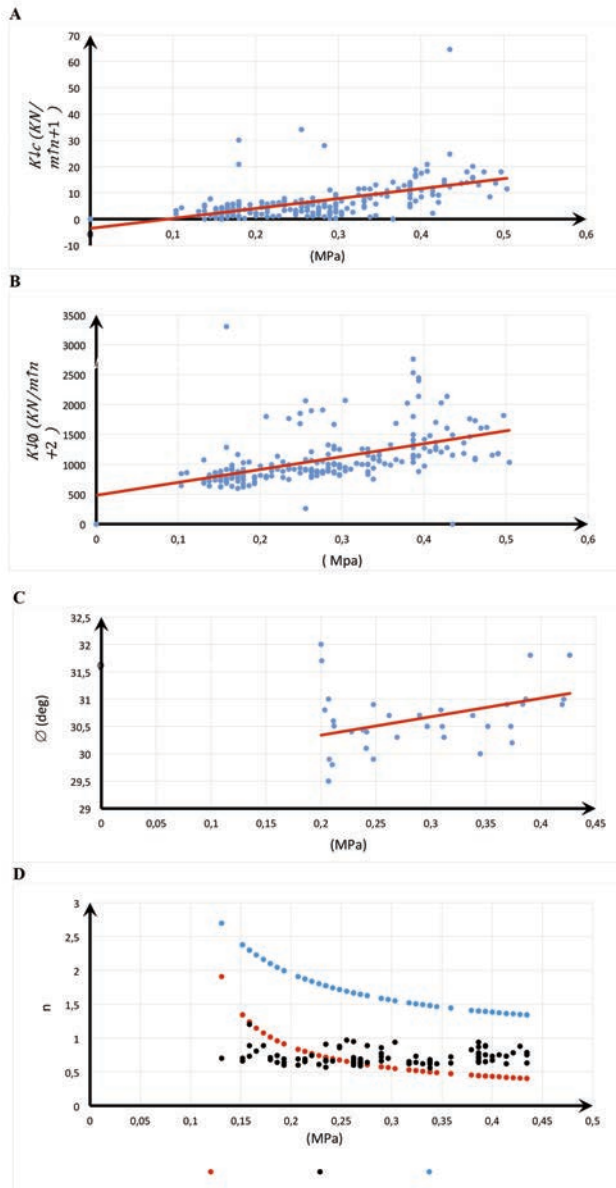


Figure 3. A) Experimental cohesion module *versus* cone index; B) experimental friction module *versus* cone index; C) experimental friction angle *versus* cone index; D) validated graph of predicted sinkage exponent *versus* the cone index for the proposed equation, Janosi's equation, and experimental data obtained from waterways experiment station.

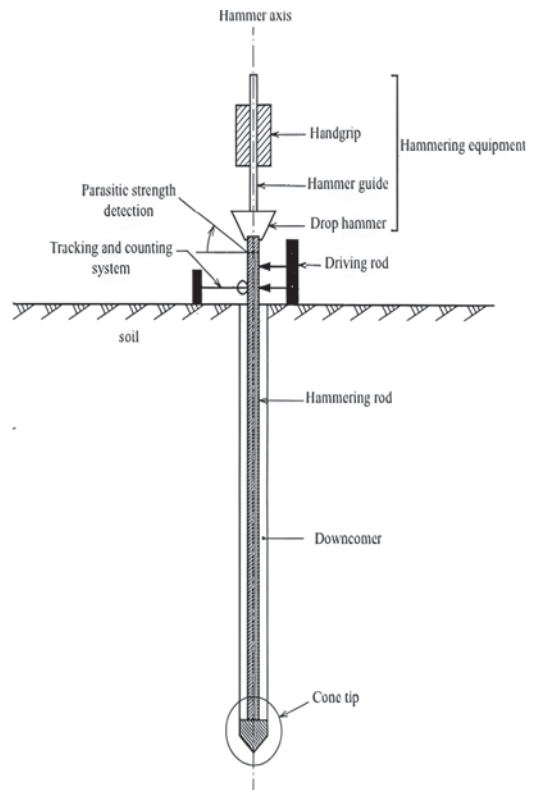


Figure 4. Schematic of a dynamic penetrometer PDR.

Determination of the parameters

In order to identify the bevametric parameters specific to the soil inside the didactical greenhouse, it is necessary to solve the proposed equation by considering the experimental data given in Figure 7A. For this reason, we will use the average of the measurements picked from ten areas in the agricultural robot pathway, as shown in Figure 7B.

It can be seen in the graph that the penetration resistance fluctuates greatly while descending to a given depth.

Let \bar{I}_{ci} be the average cone index measured at depth Z_i . It is assumed that the soil is homogeneous around Z_i . Thus, the bevametric parameters are independent of the depth.

Therefore, we can write Equation 21 in its average form, as shown in Equation 27:

$$\bar{I}_{ci} = f(K_c, K_\phi, n, \phi, c, Z_i) \tag{27}$$

This equation consists of five variables. The value of I_C measured at five depths is available; then, the system is solved. Thus, the following system is obtained:

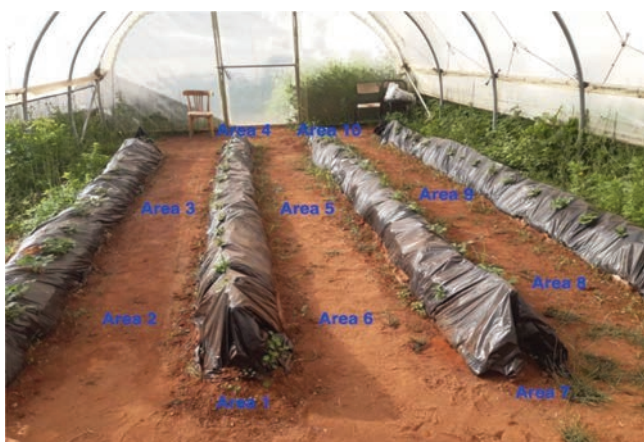


Figure 5. Measurement areas inside a didactical strawberry greenhouse.



Figure 6. Drill bit used in greenhouse ground.

$$\begin{cases} \bar{I}_{c1} = f(K_c, K_\phi, n, \phi, c, Z_1) \\ \bar{I}_{c2} = f(K_c, K_\phi, n, \phi, c, Z_2) \\ \bar{I}_{c3} = f(K_c, K_\phi, n, \phi, c, Z_3) \\ \bar{I}_{c4} = f(K_c, K_\phi, n, \phi, c, Z_4) \\ \bar{I}_{c5} = f(K_c, K_\phi, n, \phi, c, Z_5) \end{cases} \tag{28}$$

Table 1. Average dry bulk density and moisture content of the soil inside the greenhouse strawberries.

	Bulk density g/cm ³	Moisture content %
Average value	1.32	24.6

Table 2. Soil analysis table based on the experimental study inside a greenhouse using a drill bit.

Average depth (m)	Average soil texture (%)		
	Clay	Sand	Silt
0-0.5	29%	52%	19%
0.5-0.8	32.5%	50%	17.5%
0.8-1	35.5%	49%	15.5%

Table 3. Bevameter parameters using the proposed equation with the help of the experimentation inside the greenhouse with strawberries.

K_c (KN/m ⁿ⁺¹)	K_ϕ (KN/m ⁿ⁺²)	n	c (MPa)	ϕ (deg)
14.5	705.22	0.36	0.004	31.5

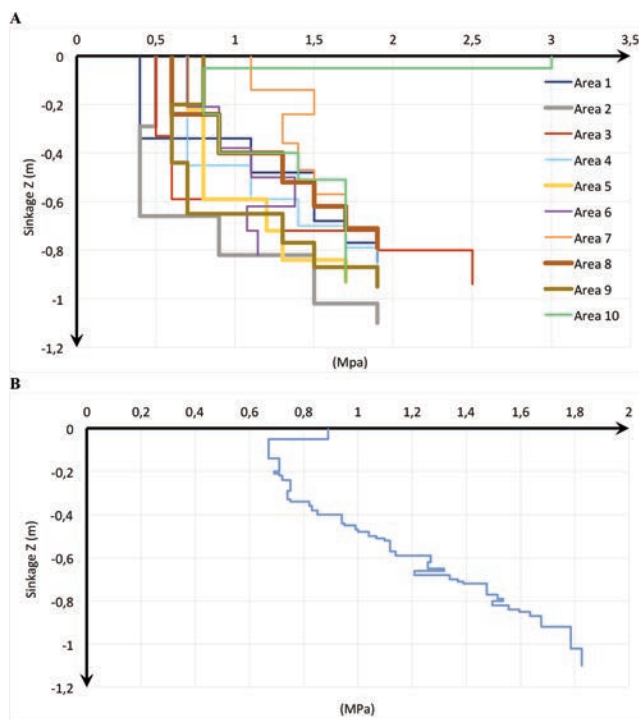


Figure 7. A) Experimental cone penetrometer measurement versus sinkage depth; B) average cone index obtained inside a didactical strawberry greenhouse versus sinkage dept.

Equation 21 is adapted to the characteristic of the cone penetrometer used in the experimentation is shown as follows:

$$I_c = 4.8 (0.57 + \tan(\theta)) \left[\frac{\frac{K_c}{n+1} ((Z + 0.025)^{n+1} - (Z)^{n+1}) + 1.15 K_\theta \left[\frac{((Z+0.025)^{n+2} - (Z)^{n+2} - 0.025(n+2)Z^{n+1})}{(n+2)(n+1)} \right]}{1.15 K_\theta \left[\frac{((Z+0.025)^{n+2} - (Z)^{n+2} - 0.025(n+2)Z^{n+1})}{(n+2)(n+1)} \right]} \right] + 0.00173c \quad (29)$$

The values of the unknowns K_c , K_θ , n , θ , c , are calculated using the Excel solver tool and given in Table 3.

The found parameters are particularly accurate in estimating the soil's bevametric parameters. Moreover, it shows compatibility with the values given in the literature. This enables us to get an overview of the nature of the soil existing in the greenhouse (clayey sand soil with many fines) for further use in the future works.

Conclusions

Bevametric parameters estimation is undoubtedly very hard to deal with in rough terrain. Therefore, these parameters are usually found using a bevameter instrument. However, this instrument is not usually available in an open environment like the agriculture field. Hence, the cone penetrometer is used. This paper provides an expression linking all bevametric parameters with a cone index measurement. The proposed expression is more optimal compared to those existing in the literature. The found expression determines all bevametric parameters inside the greenhouse with strawberries.

References

- Andrew S. 1986. Waterways experiment station, 1964. Measuring Soil properties in vehicle mobility research, strength-density relations of an air-dry sand; waterways experiment station TR 3-652, Report 1, Vicksburg, Miss. Oxford: Oxford University, 60.
- Bekker M.G. 1969. Introduction to terrain-vehicle systems. Michigan: The University of Michigan Press.
- Dong P., Wang X., Xing H., Liu Y., Zhang M. 2016. Design and control of a tracked robot for search and rescue in nuclear power plant. pp 330-335 in ICARM 2016 - 2016 International Conference on Advanced Robotics and Mechatronics.
- Geotechnical, Canadian. 1991. Literature on cone penetration testing.
- Hereid A., Eric A.C., Christian M.H., Aaron D.A. 2016. 3D dynamic walking with underactuated humanoid robots: a direct collocation framework for optimizing hybrid zero dynamics. pp. 1447-54 in Proceedings - IEEE International Conference on Robotics and Automation 2016.
- Janosi Z. 1959. Prediction of "WES Cone Index" by Means of a stress-strain function of soils. Laughery.
- Johnson C.E., Grisso R.D., Nichols T.A. 1983. Shear measurement for agricultural soils - a review. Am. Soc. Agric. Engine. 30:2-5.
- Li Y., Yan A.Y., Cheng J., Tian Y., Liu R. 2017. An agile assistant robot integrating operation and rolling locomotion. Industr. Robot 44:114-26.
- Livneh M., Noam A.L. 2013. The use of the dynamic cone penetrometer for quality control of compaction operations. Int. J. Engine. Res. Africa 10:49-64.
- Ma'arif A., Rahmaniar W., Vera M.A.M., Nuryono A.A., Majdoubi R., Çakan A. 2021. Artificial potential field algorithm for obstacle avoidance in UAV quadrotor for dynamic environment. pp 184-189 in 2021 IEEE International Conference on Communication, Networks and Satellite (COMNETSAT). doi:10.1109/COMNETSAT53002.2021.9530803
- Majdoubi R., Masmoudi L. 2021. Eco-design of a mobile agriculture robot based on classical approach and FEM criteria. pp 978-82 in Proceedings - IEEE 2021 International Conference on Computing, Communication, and Intelligent Systems, ICC-CIS 2021.
- Majdoubi R., Masmoudi L., Bakhti M., Jabri B. 2021. Torque control oriented modeling of a brushless direct current motor (BLDCM) based on the extended park's transformation. J. Eur. Syst. Automat. 54:165-74.
- Majdoubi R., Masmoudi L., Bakhti M., Elharif A., Jabri B. 2020. Parameters estimation of bldc motor based on physical approach and weighted recursive least square algorithm. Int. J. Electr. Computer Engine. (IJECE) 11:133-45.
- Majdoubi R., Masmoudi L., Elharif A. 2021. Torque control using metaheuristic optimization for optimal energy consumption of a BLDCM. 2021 IEEE International IOT, Electronics and Mechatronics Conference, IEMTRONICS 2021 - Proceedings.
- Majdoubi R., Masmoudi L. Elharif A. 2022. Explicite model of a wheel-soil interaction over a rough terrain using terramechanics low. pp 1-7 in 2022 IEEE International IOT, Electronics and Mechatronics Conference (IEMTRONICS). doi: 10.1109/IEMTRONICS55184.2022.9795754
- Mei M., Chang J., Li Y., Li Z., Li X., Lv W. 2019. Comparative study of different methods in vibration-based terrain classification for wheeled robots with shock absorbers. Sensors (Switzerland) 19:5.
- Molari G., Mattetti M., Walker M. 2015. Field performance of an agricultural tractor fitted with rubber tracks on a low trafficable soil. J. Agric. Engine. 46:162-6.
- Next-Generation. 2018. NATO reference mobility model (NRMM) development. Vol. 323.
- Noriyasu A., Kanzaki R. 2017. Using insects to drive mobile robots - hybrid robots bridge the gap between biological and artificial systems. Arthropod Struct. Develop. 46:723-35.
- Nowatzki L.L., Karafiath E.A. 1978. Soil mechanics for off-road vehicle engineering. Trans. Tech Publ., April.
- Rios S.A., Fleming A.J., Yong Y.K. 2017. Miniature resonant ambulatory robot. IEEE Robot. Automat. Lett. 2:337-43.
- Rohani B., Baladi G.Y. 1981. Correlation of mobility cone index with fundamental engineering properties of soil: final report. Washington, DC: GPO.
- Ruiz A., Blandón A. 2015. Covariance structure analysis on health-related indicators in elderly people at home, focusing on subjective sense of health. Vol. 3.
- Station, Waterways Experiment. 1964. Strength-moisture-density relations of fine. Grain soils in vehicle mobility research waterways experiment station TR 3-639, Vicksburg, Miss. Waterways.
- Vesic A.S. 1981. Expansion of cavities in infinite soil mass. J. Soil Mechan. Found. Divis. ASCE, Vol 98, SM3. Proc. Paper 8790, March 1972.
- Wright D.D., Wright A.J., Boulter T.D., Ashlie A.B., Brian C.S., Zaugg B., Jeff H.P., Ha L., Ta B.T., Randall J.O. 2017. Optimization of transversal phacoemulsification settings in peristaltic mode using a new transversal ultrasound machine. J. Cataract Refract. Surg. 43:1202-6.